

Set up of a Schlieren Flow Visualization Device

Author: Pol Sopeña i Martínez

Facultat de Física, Universitat de Barcelona, Martí i Franquès 1, 08028 Barcelona, Spain.

Abstract: For many people seeing means understanding because it is the most direct way of verifying. Thus, seeing phenomena into transparent media represents a challenge which needs to be solved. The schlieren technique is a method that allows to see changes in the refractive index of transparent materials when a density gradient is established. In this paper a schlieren visualization device will be put together and characterized. Different arrangements were assembled in order to discuss which is the optimum setup. Several aspects as type of light source, focal length or knife-edge cutoff are taken into account. Ultimately, the device was tested in extreme conditions when it was used to visualize a sound wave produced by an electric spark. This allowed us to determine its speed and, therefore, corroborate that the visualized perturbation indeed corresponds to a sound wave.

I. INTRODUCTION

The first people who saw inhomogeneities in transparent media probably did it by what is now known as shadowgraphy. For instance, when light from the sun goes through the surface of a shallow river and creates ripple-like shadows on its bed. However, what we know as schlieren technique was not reported until the 17th century by R. Hooke and C. Huygens [1]. Later on, J.P. Marat was the first person who drew and observed flow in fluids [2]. But it was not until the 19th century that A. Toepler [3] studied the phenomenon with great detail. He used the first knife-edge cutoff, other than the pupil's eye, and named it schlieren, which means 'optical inhomogeneities in glass' in German. Nowadays, it is widely used to explore shock wave motion and fluid dynamics, such as noise generation in pulsating air jets or density variations in water due to vortexes.

Light travelling through transparent media slows its speed from c (light speed in vacuum) to v , letting us define the refractive index $n = c/v$. This index is different for all materials and strongly depends on their density. For gases this relation is $n = k\rho + 1$, where ρ is the density and k is the Gladstone-Dale coefficient, different for each gas. If we consider that our gas satisfies the perfect-gas state equation, $p = \rho RT$ where p is its pressure, R is the specific gas constant and T is its temperature; it is observed that temperature or pressure variations will lead to a change in the refractive index. As well, the Gladstone-Dale coefficient is not constant but increases slightly for increasing wavelengths λ [4].

In the following, we will derive how these index variations interact with light. Let us suppose a planar light wavefront that travels along the z axis in a medium of refractive index n , where we consider a right-handed Cartesian x, y, z coordinate system. When this medium suffers a refractive index variation from n_1 to n_2 along the z axis, rays will bend and the wavefront will change direction. This change in direction describes an angle $\Delta\epsilon$ respect to the z axis in the y direction. Thus, by knowing the speed variation $v_2 - v_1$ and considering the angle to be small, one can write:

$$\Delta\epsilon = \frac{\Delta z}{\Delta y} = \frac{(v_2 - v_1)\Delta t}{\Delta y} = \frac{c(1/n_2 - 1/n_1)\Delta t}{\Delta y} \quad (1)$$

where Δy is the original wavefront length. The differential time Δt is the time for the light to travel from the point with index n_1 to the point with index n_2 when the medium is unaltered.

$$\Delta t = \frac{\Delta z}{v} = \Delta z \frac{n}{c} \quad (2)$$

Combining eq.(1) and eq.(2) and assuming that the perturbation led to a very small change in n , the next relation holds:

$$\frac{d\epsilon}{dz} = \frac{1}{n} \frac{dn}{dy} \quad (3)$$

Assuming a perturbation of length L and integrating eq.(3) we obtain that a refractive index variation in the y axis leads to a deflection angle ϵ_y of the rays that otherwise would be parallel to the z axis:

$$\epsilon_y = \frac{L}{n} \frac{\partial n}{\partial y} \quad (4)$$

Thus, any refractive index variation in the $x-y$ plane of a transparent object will result in the deflection of the rays that travel through that object. All along the previous derivation we have assumed a bidimensional gradient field and disregarded any variations along the z axis.

Let us now suppose a setup like the one presented in Fig.1 in order to explain the underlying principle of the schlieren technique. Let a point light source be in the object focal point of a converging lens. Thus, all rays emerging from the lens are parallel. Then, a second converging lens collects all rays on its image focal point, where a knife-edge cutoff is placed at a height that it almost intersects the beam completely. The medium to study, or schlieren object, has to be placed between the lenses. Finally, a camera or screen is placed in the image plane of the schlieren object in order to visualize the resulting image.

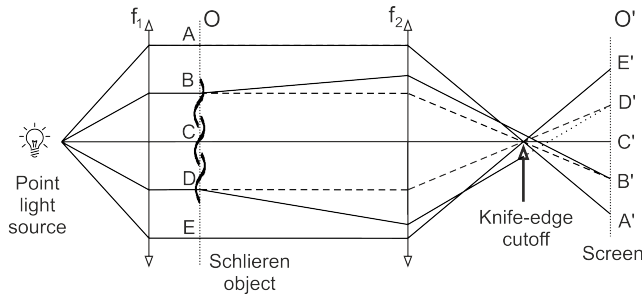


Figure 1: Principle of operation of the schlieren technique.

As observed in Fig.1, when there is no alteration in the schlieren object all rays focalize at the same point and pass freely through the cutoff. Hence, an even illumination image is projected on the screen. However, let us assume that the schlieren object suffers a refractive index variation. Now, rays that were parallel to the optical axis are deflected according to eq.(4) and as displayed in Fig.1. Thus, rays emerging from B and D are deflected upwards and downwards respectively, for example, and no longer converge in the focus of lens f_2 . By placing the cutoff in the focal point, all rays that are deflected downwards are cut out and cannot reach the screen, leaving a shadow on it. Thus, when there is a perturbation in the schlieren object and the knife-edge is in place we are able to obtain a binary image (bright and dark) where some of the deflected rays are cut out and others pass freely.

Nevertheless, real light sources are finite, no matter how small, and act as the sum of countless point light sources. Therefore, the obtained image in an actual experiment is not binary but gray-scale. This is due to the combination of many rays following different paths and crossing the cutoff at different heights. So, when the image is composed by summing all the rays, the illuminance level will depend on the amount of none-cut-out rays [5].

There are two main features which define how the gray-scale image looks like: the sensitivity and the measuring range. Sensitivity is the ability to detect changes in the refractive index of the media, so the minimum perceptible refractive index variation. The measuring range is the range of angles over which an illuminance alteration can be measured. In [4] it is seen that sensitivity is proportional to the focal length of the second lens and inversely proportional to the height of the beam that avoids the cutoff. Besides, it is pointed out that sensitivity and measuring range are inversely proportional to each other. Thus, given a certain focal length for the second lens, the knife-edge will be placed at the right height so that both sensitivity and measuring range are as high as possible. Moreover, to detect small changes in the refractive index of the schlieren object a great separation between the two lenses is required. A problem concerning the illumination arises when placing the knife-edge: the higher the cutoff edge, the less the illuminance. Thus, an intense light illumination system is required to see clear images and to avoid the loss of light.

Aiming to set up a schlieren visualization device and check its performance, we set up a dual-field-lens schlieren arrangement [6]. It essentially corresponds to the sketch in Fig.1, yet the screen was replaced by a recording camera and the light source required a condenser to avoid the loss of light and an iris diaphragm to simulate a point light source.

II. EXPERIMENTAL SETUP

The core of the setup was composed of a light source and a collimating system, an iris diaphragm, which aperture worked as point light source, two converging lenses with a focal length of 150 mm, a horizontal blade from an utility knife as cutoff and a CCD camera.

Three different lamps were tested: a conventional tungsten halogen lamp of 500 W, a xenon arc lamp of 200 W and a tungsten halogen fiber light source of 150W. The halogen lamp is cheap and available, which makes it a good option to build a simple setup. Besides, it offers a white-yellowish colour-light of 3000 K. Nonetheless, the dimensions of the incandescent filament are similar to the iris aperture, which means that its image will propagate through the setup if the iris is placed close to it; this will result in the superposition of the filament in the pictures, which would be clearly detrimental for the correct visualization of the flow. That can be solved by using a diffuser; however, there will be a substantial loss of light. On the other hand, the xenon arc lamp offers 10 to 100 times more luminous output than the tungsten-filament lamp [4]. Its light corresponds to a temperature of 6000 K which mimics the greenish-white hue of the Sun. The major inconvenience is the heating up and the emission of UV radiation which might be both harmful to the schlieren object. In order to focalize the light from both the lamps on the iris, a lens or a collimator was used. Finally, the fiber halogen lamp, which has a colour temperature of 3200 K, has less power but it has a built-in collimator and optic fiber which avoid the loss of light and make it brighter. Unlike the other lamps this one does not require a collimator or diffuser and can be placed directly before the iris diaphragm.

Depending on the illumination system and the phenomenon to study we used two different cameras which allowed us to control different parameters. The high-speed CCD camera (S-PRI F1, AOS Technologies) is a continuously-recording camera capable of recording at 1000 fps. In spite of its high performance, this camera cannot be synchronized with events that require less than 1 ms precision because it is constantly recording. The alternative is an intensified CCD camera (Animator-V1, ARP France), which uses a microchannel plate (MCP) as intensifier and has a minimum exposure time of 50 ns. This camera can only take one image every time it is triggered, yet it can be synchronized up to the nanosecond, which makes possible the visualization of very fast repetitive events through a stroboscopic strategy.

- Halogen lamp - Configuration 1

When using the halogen lamp we placed a single 50 mm focal-length lens as condenser in order to collect the light onto the iris and a GRIT-120 diffuser attached to it. The condenser lens was 110 mm to the right (right and left positions are given based on the sketch of Fig.1.) of the tungsten-filament. Then, the iris was placed 84 mm to the right of the condenser lens. The first field lens was placed so that its object focal point lays in the diaphragm. Thus we obtain a parallel-ray beam travelling through the schlieren object and onto the second field lens. These two lenses needed to be as much separated as possible in order to obtain maximum sensitivity. In our setup their separation was set to 360 mm. The schlieren object was placed close to the object focal point of the second lens, to its left. Finally, the knife-edge cutoff was placed at 150 mm to the right from the second lens, at the image focal point. Its height determined the contrast of the observed gray-scale image, thus, it had to intersect the beam, but not totally. With all the system well aligned the high-speed camera was placed after the cutoff. The position of the cutoff was accurately determined by moving it back and forth so that when the cutoff was risen the illumination of the resulting image faded homogeneously. It had to be taken into account that the higher the cutoff the higher the contrast but the lower the illuminance.

- Arc lamp - Configuration 2

In this configuration the halogen lamp was replaced by the arc lamp. The particular model of lamp used in our setup propagated an image of the internal electrodes. To solve that a GRIT-120 diffuser was placed at the exit of the lamp. Instead of using one lens, a collimator of two lenses was assembled. The first lens ($f=150$ mm) was located 12 mm to the right of the diffuser, the second lens ($f=75$ mm) was 65 mm to the right of the first lens and the iris was 80 mm to the right of the second lens. This arrangement allowed to focalize more light onto the iris. Likewise, the rest of the schlieren arrangement continued unaltered.

- Fiber lamp - Configuration 3

In this configuration the fiber lamp was used. Since this lamp already included a built-in collimating system and an optic fiber, no condenser was required. Thus, the optic fiber was directly attached to the iris diaphragm. The following part of the schlieren setup remained the same.

Each configuration was optimized to obtain the best possible results. First the light source was placed, then the collimator and the diaphragm and, finally, the schlieren piece. The accurate alignment of the lenses was essential in order to obtain even illumination as well as to avoid the loss of light. The distance between the field lenses was the furthest given the dimensions of the optical bench. In order to obtain high sensitivity and high

resolution the diaphragm aperture was set at 0.7 mm. The camera settings were adjusted so that images were both bright and well focused.

III. RESULTS AND DISCUSSION

To test the proper performance of each configuration, different schlieren objects were visualized. The effects discussed in the forthcoming sections and presented in the figures of this report are best appreciated in their corresponding movies. The reader can find the complete collection in <https://www.youtube.com/user/PSMschlierenTFG>.

A. Setup Characterization

In order to test the capabilities of the setup we considered two different situations. Firstly, gas coming out of a lighter. When the gas comes out, the air density varies because there is a high concentration of gas from the lighter. Thus, the gas jet should be detectable. In second place, air from a heat gun, a device similar to a hair-drier but with a higher power. When the device is on the variation of the refractive index due to the temperature gradient and the air flow should be detectable.

- Configuration 1

In Fig.2 results for the first configuration setup are presented. Images in the upper row (Fig.2 Aa, Ab, Ba and Bb) have no cutoff, so no perturbation is observed when the device is on. However, for the heat gun some wavy-shadows appear, though they are barely perceptible. This is due to the relatively small diameter of the used lenses (36 mm) which worked as cutoff. Red and blue coloured regions appear due to chromatic aberration when the cutoff is placed for images in the lower row (Fig.2 Ac, Ad, Bc and Bd) [7]. The colour gradient direction corresponds to the cutoff translation. The air flow of the heat gun is visualized and dark and bright wavelike regions are created. Furthermore, it can be seen how the gas of the lighter rises up in the air and then to the right, probably as consequence of a draught.

- Configuration 2

Same as before, in Fig.3 when there is no cutoff no gray-scale image is produced for the lighter but a pattern can be appreciated for the heat gun. Unlike the arrangement of the first configuration, now the coloured regions are green and blue because the arc lamp emits at a different colour temperature. When the knife-edge is risen the gray-scale image appears clearly and the flow of gas from the lighter is more visible. Thus, by changing the lamp and the collimator the system becomes brighter and is more sensitive, though in the frozen images is barely perceptible.

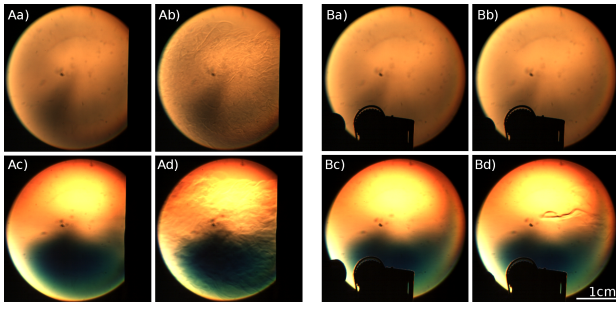


Figure 2: Heat gun A) and lighter B) for Configuration 1. The device responsible for the schlieren object was set to be off with no cutoff a), to be on with no cutoff b), to be off with cutoff c) and to be on with cutoff d).

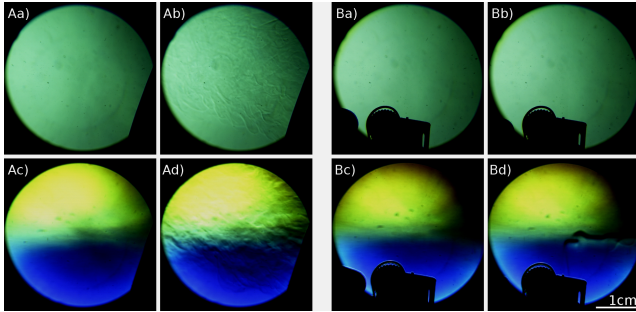


Figure 3: Heat gun A) and lighter B) for Configuration 2. The device responsible for the schlieren object was set to be off with no cutoff a), to be on with no cutoff b), to be off with cutoff c) and to be on with cutoff d).

- Configuration 3

The last configuration did not require a collimator and light was simply directed onto the diaphragm. Snapshots in Fig.4 show how that allowed to obtain brighter images. When no cutoff is present no pattern can be observed; however, it can be slightly observed in the movies. Unlike before, the system is clearly more sensitive when the cutoff is risen, thus, the air flow is dramatically contrasted by darker and brighter regions. The gas stream is likewise clearly visible. Because the colour temperature is similar to that of the first configuration the coloured regions are again red and blue.

This study proves that the implemented schlieren setup is feasible for gas flow visualization, being Configuration 3 the one which provides with the optimum results.

B. Proof of concept

After having characterized the schlieren device and determined the optimum configuration, a more challenging instance is considered. Knowing that an electric spark produces a sound wave, which is a pressure variation

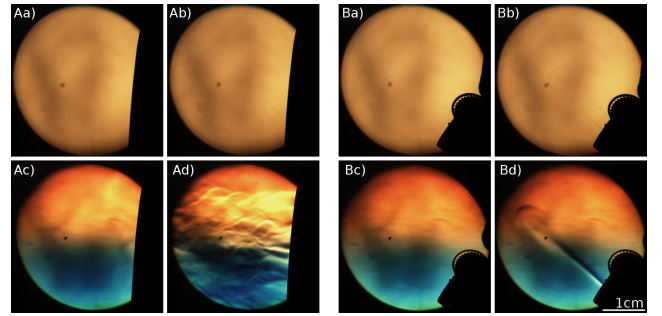


Figure 4: Heat gun A) and lighter B) for Configuration 3. The device responsible for the schlieren object was set to be off with no cutoff a), to be on with no cutoff b), to be off with cutoff c) and to be on with cutoff d).

propagated through air, we aimed to visualize that phenomenon [8]. Since sound propagation is a much faster phenomenon than any of the ones used in the previous characterization, a synchronism system between the spark generation and the image acquisition will be now required.

A spark lamp (Nanolite) was placed in the schlieren object plane. This lamp produces an electric spark of only 22 ns. In order to obtain clear snapshots and taking into account the field of vision (3 cm) and the speed of sound (~ 340 m/s), exposure times of the order of μs were required. The intensified camera Animator-V1 satisfied these working conditions and could be adequately synchronized, which would be otherwise impossible with the high-speed camera previously used.

In Fig.5 the synchronism scheme is presented. First of all, signal S1, provided by a pulse generator, triggered the spark. Then, two simultaneous pulses were necessary, one to trigger the MCP (S2) and another to acquire the image (S3). The delay between S1 and S2-S3 had to be at least of $3.27 \mu\text{s}$. However, this delay time was variable, being $3.27 \mu\text{s}$ the required delay to capture the spark ignition, and longer delays were considered in order to take snapshots of the propagating wavefront. The variable delay is represented in Fig.5, where t is the time between the spark and acquisition time. The corresponding stop-action movie is presented in Fig.6. The illumination system did not require synchronization because it is a continuous light source. All images were taken with $0.5 \mu\text{s}$ exposure time to avoid blurriness and still obtain clear images with enough brightness.

It can be observed in the following images of Fig.6 how a circular shadow, which corresponds to the sound-wave front, propagates upwards. The first image corresponds to the spark generation ($t=0 \mu\text{s}$). In both first and second image nothing can be detected because the perturbation has not yet emerged from the electrodes cage. Darker regions attributed to a temperature gradient in air are observed beneath the perturbation front. In order to determine the speed of the perturbation we can plot its distance from the surface of the lamp versus the elapsed

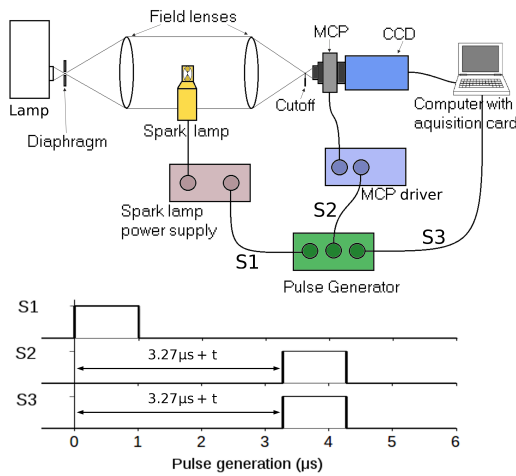


Figure 5: Scheme of the synchronization system.

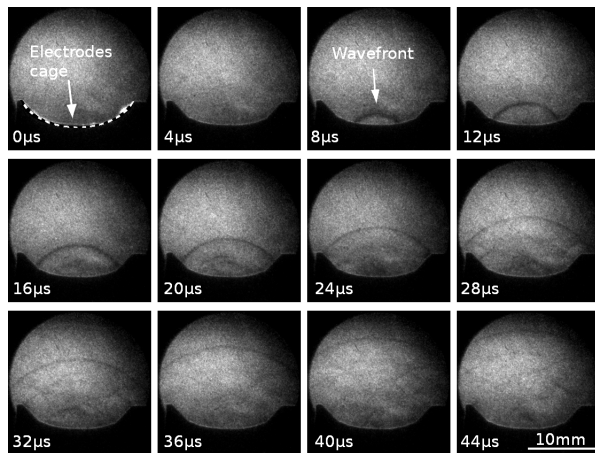


Figure 6: Images of the sound wave propagating upwards; in the bottom of the frames the delay between the spark ignition and the acquisition of the image is indicated. A dashed line contouring the electrodes cage is drawn in the first image.

time, as presented in Fig.7.

From the collected data it is observed that all data points are aligned, which indicates that the propagation advances at a constant speed. When performing a linear fit to the data sets a speed of 360 m/s was obtained,

which matches fairly well the speed of sound in air at room temperature.

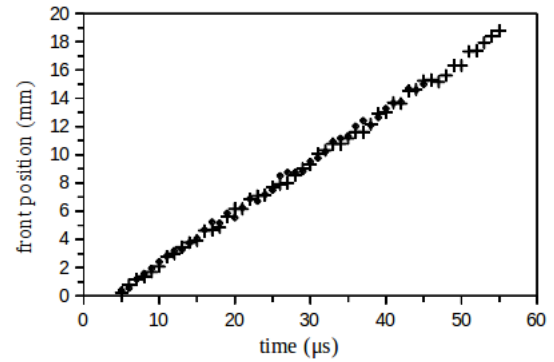


Figure 7: Position of the sound wavefront respect to the edge of the electrodes cage versus time. Two data sets (crosses and circles) were acquired.

IV. CONCLUSIONS

The schlieren technique has been proved feasible to visualize transient flows in transparent media by setting up a double-field lens arrangement. It has also been shown that enhancing the illumination system by placing a collimator and choosing a more luminous light source more contrasted images were obtained, thus corroborating that a brighter lamp is needed to improve the quality and sensitivity of the images. Finally, the setup has been proved to be sensitive enough to detect and track a sound wave generated by an electric spark. The visualization has showed that the generated perturbation propagated at a speed of 360 m/s which indicates that it indeed corresponds to a sound wave.

Acknowledgments

The advisory work of Dr. P. Serra is greatly acknowledged, as well as the assistance of Dr. J.M. Fernández-Pradas in the laboratory. Many thanks to my laboratory colleagues and my family and friends.

[1] Rienitz, J. "Schlieren experiment 300 years ago". *Nature* **254**: 293-295 (1975).
 [2] Marat, J.P. "Recherches physiques sur le feu". Cl. Ant. Jombert, Paris (1780).
 [3] Krehl, P. and Engemann, S. "August Toepler — The first who visualized shock waves". *Shock Waves* **5**: 1-18 (1995).
 [4] Settles, G.S. *Schlieren and Shadowgraph Techniques: Visualizing Phenomena in Transparent Media*. (Springer-Verlag, Heidelberg, NY, 2001).
 [5] Mazumdar, A. "Principles and techniques of schlieren

imaging systems". Columbia University, NY. Technical Report CUCS 016-13 (2011).
 [6] Neubauer, W.G. and Dragonette L.R. "A schlieren system used for making movies of sound waves" *Journal of the Acoustical Society of America* **49**: 410-411 (1971).
 [7] Hays, G.E. "A Color Schlieren System for High-Speed Photography". *SMPTE Journal* **66**: 355-356 (1957).
 [8] Spenceley, B.J. and Dakin, P. "Velocity of sound in air using schlieren techniques". *Am. J. Phys.* **33**: 51-54 (1965).